SAND2012-7270C

Methodology for creating nonaxisymmetric WECs to screen mooring designs using a Morison Equation approach

Diana Bull
Water Power Technologies
Sandia National Laboratories
Albuquerque, NM 87185
Diana.Bull@sandia.gov

Paul Jacob
Jacob Technologies
Sugarland, TX 77478
pj@jtec-tx.com

***Abstract*—This paper outlines a methodology to derive the rigid body motions from Morison Equation forces for a floating Backward Bent Duct Buoy (BBDB). This Wave Energy Converter (WEC) is a particular style of Oscillating Water Column (OWC). The methodology details how to decompose the BBDB into a series of 'hydrodynamic bodies' to account for inertial and viscous effects, 'structural bodies' to account for structural mass and inertia, and freely flooding bodies to account for the time dependent variation of entrained water mass in the OWC of the device. Separating these effects allows for independent treatment of the phenomena being modeled and for an easily adaptable WEC model. Because effects of the PTO can be eliminated when considering extreme conditions, OrcaFlex, a validated mooring time domain solver, is applied to this problem. Thus coupled analysis between the proposed mooring system design and the BBDB dynamic response allows for mooring system component specification. Due to the dependence of Morison Equation force magnitudes on empirically derived drag coefficients, the paper concludes with a study quantifying the effect of drag coefficient magnitude on survival mooring loads.**

Key Words: WEC, BBDB, OWC, OrcaFlex, mooring, Morison Equation, extreme wave environment

I. Introduction

The cost of a Wave Energy Converter (WEC) mooring system is a significant portion of the total installed cost of a WEC device [1]. Consequently, it is important to obtain realistic load predictions early in the design process so that mooring system components can be realistically sized. It is also important that the analysis procedure used to design the mooring system be easily adaptable so that mooring configurations can be modified and updated without major time and expense.

The moored WEC studied in this paper is a Backward Bent Duct Buoy (BBDB), a particular style of an Oscillating Water Column (OWC) WEC first proposed by Masuda [2]. The BBDB is a floating OWC device that consists of an air chamber, an L-shaped duct, buoyancy modules, and a power take-off (PTO) composed of an air turbine and generator. Power is produced by forcing air to flow through the PTO/turbine. Figure 1 illustrates the main components of a BBDB [3].

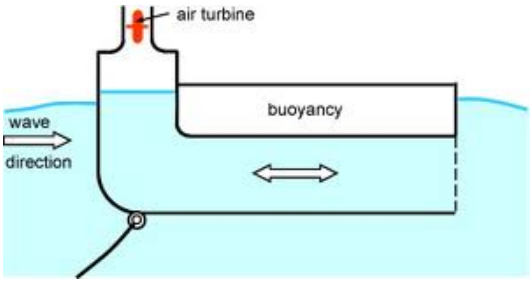

Fig. 1. Illustration of a BBDB [3].

The floating BBDB design capitalizes on the coupling between the motion of the structure and motion of the free surface contained within the structure. This coupling can increase the relative motions of the free surface and expand the frequency range over which good power conversion occurs. In theory, the BBDB has a higher primary conversion efficiency when compared to other OWC's [4].

Extreme wave environments typically drive the sizing of mooring system components due to the relatively large hydrodynamic loads that they generate. Thus, the mooring design must arise from analysis in this environment. The extreme wave environment is often sufficiently large that the translational and rotational motions of the WEC are on the limits of applicability for classic (radiation/diffraction) frequency domain potential flow solvers. Thus, it is preferable that the WEC's response to large amplitude waves should be derived from an alternative to frequency domain potential flow solvers.

The flow conditions around the WEC can be characterized by the diffraction parameter, $\frac{\pi L}{\lambda}$, and the waveheight to characteristic length ratio, $\frac{H}{L} \alpha \frac{KC}{\pi}$, where λ is the wavelength, L is the characteristic body length, H is the waveheight, and KC is the Keulegan Carpenter number. Chakrabarti [5] reasoned that viscous drag dominates a structure's motion when the diffraction parameter is small and the waveheight to characteristic length ratio is large. If these conditions are met, then Morison's Equation, an empirical force formulation that is valid when drag is important to the dynamics of a structure, can be used to effectively describe the wave-structure interactions.

This paper outlines a methodology to create a BBDB model using elemental inertia, hydrostatic, and hydrodynamic characteristics that requires only Morison Equation forces to resolve the device rigid body motions in six degrees of freedom (6-DOF). This modeling approach for the WEC in turn allows for characterization of the expected survival mooring loads and evaluation of a mooring design. The lumped bodies that represent the BBDB include a series of 'structural bodies' to account for structural mass and inertia, 'freely flooding bodies' to account for the time dependent variation of entrained water mass in the OWC, and 'hydrodynamic bodies' to account for inertial and viscous effects. Separating individual responses allows for each to be treated independently and in a manner that is consistent with the phenomenon being modeled.

The common survival strategy for a WEC when subjected to the large forces and motions in an extreme wave environment is to stop producing power to protect the PTO. The PTO of the BBDB can be easily protected in extreme environments through a pressure relief system capable of venting the air chamber to the outside. Eliminating the PTO effects from the survival-condition response allows BBDB motions in survival conditions to be assessed using validated coupled mooring time domain solvers that are typically used in the offshore marine and petroleum industries. The program OrcaFlex [6] is used in this case as it readily has functionality to handle the coupled analysis between the mooring system and the WEC dynamic response.

The general discretization methodology used to develop the BBDB is outlined in Section II of the paper. Section III presents a case study using the analysis procedure. The case study evaluates the mooring design loads as well as highlights the importance of empirical drag coefficient values with a parametric study.

The methodology to calculate 6-DOF motions from Morison's Equation is not specific to a particular WEC design. The discretization method is a strategy that can be used to design any WEC subject to the general limitation of the method, namely the applicability of Morison's Equation and the impact of the PTO on the WEC response in extreme conditions.

II. DISCRETIZATION METHOD

A model of the BBDB OWC was developed using an array of 6-DOF lumped bodies representing

- buoyancy distribution,
- freely flooding bodies that account for the time-dependent variation of entrained water mass, and
- hydrodynamic characteristics that account for inertial and viscous effects.

The array of lumped bodies is then attached to a reference body that acts as the integrand of the loading effects. Separating individual responses allows for each to be treated independently and in a manner that is consistent with the phenomenon being modeled; for example the bodies representing the buoyancy distribution will not be assigned mass or hydrodynamic properties, they will only be assigned volumes.

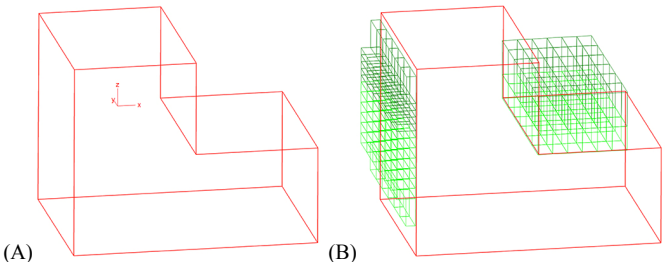

Fig. 2. Structural (A) and buoyancy (B) bodies: OrcaFlex representation.

A. Structural Bodies

A single discrete body located at the structural mass center of the device could be used to represent the structural mass and inertia of the device if these characteristics were available from a solid 3-D model. A structural body of this type is shown in red in Figure 2A. Alternatively, a similar discretization method to the one presented for the buoyancy distribution below could be used to discretize the mass distribution. In this case, the discretized mass elements would allow the program to calculate both the center of mass and the mass moments of inertia without having to know these a priori from a 3-D solid model.

The lumped bodies representing the buoyancy distribution account for the time dependent variation in the water plane area and hence the time dependent buoyancy. The bodies representing the buoyancy distribution determine the buoyant force on the basis of wetted volume and water plane area as a function of the instantaneous draft (in z axis), pitch (x–z rotation) and roll (y–z rotation) of the body. Consequently, the buoyancy bodies are discretized in both the x and the y directions. The overall buoyancy loads are calculated as:

$$B_z = \sum_{j=1}^{N} \rho g V_j \tag{1}$$

$$MB_x = \sum_{j=1}^{N} \left[(\rho g V_j) x_j \right] \tag{2}$$

$$MB_y = \sum_{j=1}^{N} \left[(\rho g V_j) y_j \right] \tag{3}$$

where N is the number of discrete buoyant bodies used to idealize the OWC structure, ρ and g are density and gravity, V_j is the volume of the jth buoyant body, and x_j/y_j are the horizontal distances between the reference body and the center of each discrete body.

The total buoyant force is a function of submergence, thus the discretized buoyant bodies represent the full height of the structure. The properties are such that they match the equilibrium conditions, i.e., the total buoyant force matches the total weight of the device at the operating draft. These bodies are shown in shades of green in Figure 2B. The light green bodies are the equilibrium submerged buoyant bodies and the dark green bodies represent the superstructure above the still water. The properties of both sets (light and dark green) are the same.

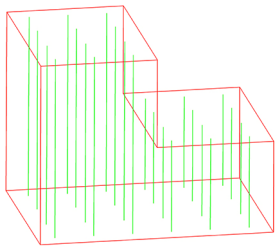

Fig. 3. Freely flooding bodies: OrcaFlex representation.

B. Freely Flooding Bodies

A unique aspect of the BBDB from other WEC types is the entrained water column. The time-dependent entrained water mass of the OWC is an important contributor to the total forces acting on the device. In diffraction theory, the entrained water mass is included in the added mass parameter calculated from the radiation potential for each mode of motion. For this representation of the device in extreme conditions, the amplitudes of motion will be large. Consequently, the small motion entrained water mass values are invalid. Because this is a survival condition, it is assumed that the PTO is disengaged from the system and hence the height of water in the BBDB is equal to the free surface height outside of the BBDB. Thus, a method to model this aspect has been developed through the incorporation of freely flooding bodies.

The height of water in the freely flooding bodies is determined by the free surface height of the surrounding wave because the air chamber is assumed vented to the outside. Because the BBDB is free to move in all 6-DOF, the freely flooding bodies must also be discretized so that pitch (x–z rotation) and roll (y–z rotation) motions of the body will be captured in the internal water column. The discretizations in the x-direction and y-direction accounts for the affect of the volume of entrained water on pitch and roll response, respectively.

The freely flooding body diameter is set by the entrained water volume at equilibrium and the bodies extend the full height of the device. The instantaneous volume of trapped water is calculated from the height of water in the bodies and inner diameter of the bodies. Figure 3 shows the central axis of the freely flooding elements in green.

C. Hydrodynamic Bodies

Morison's Equation in its extended form for a moving body is used to calculate the translational hydrodynamic forces in for each discrete body in the WEC idealization:

$$f_i = f_{inertial_i} + f_{drag_i} = \left(\rho V \ddot{r}_{fluid_i} + \rho C_{a_i} V \ddot{r}_i\right) + \frac{1}{2}\rho C_{D_i} A_i \dot{r}_i |\dot{r}_i| \quad (4)$$

where ρ is the density of water, V is the volume of the structure, $\ddot{r}_{fluid}$ is the acceleration of the fluid, C_a is the added mass coefficient, $\ddot{r}$ is the relative acceleration of the structure, C_D is the drag coefficient, A is the area on which the drag force is acting (perpendicular to local flow direction), $\dot{r}$ is the relative velocity of the structure, and the subscript i refers to each of the three translational degrees of freedom. The velocity term includes a component of velocity due to steady state current as well as a component from the instantaneous water particle velocity due to wave loading.

Consistent with the overall modeling scheme, the 'hydrodynamic bodies' are also an array of discrete bodies distributed over the volume of the WEC. The hydrodynamic bodies have no mass or volume. However, they are assigned elemental hydrodynamic properties of area and volume (see Eq. 4).

The inertial force in Eq. 4 is the sum of the Froude-Krylov force $\rho V \ddot{r}_{fluid}$ and the added hydrodynamic mass $\rho C_a V \ddot{r}$. The Froude-Krylov force is readily calculated, whereas the added mass must be estimated to obtain the inertial force. The added mass coefficient from potential flow solvers cannot be used because the entrained water mass is already accounted for in the freely flooding bodies. Thus, a method to estimate the total nonentrained added mass is necessary. This value can be approximated by assuming a hemisphere of water is moved in each translational direction with the body (only a hemisphere is used because the entrained water mass is accounting for the "other" side of the sphere).

The area that the drag force is acting on and the drag coefficient must be specified in addition to the empirically derived added mass terms. Drag coefficients are well understood for steady flow past various geometries. However there is considerably less research for devices that have large oscillation amplitudes in unsteady flow. The research that has been conducted is for damping plates that are specifically used to decrease the response amplitude of floating structures. These studies quantify the drag coefficient as a function of the dimensionless Keulegan-Carpenter (KC) number given by:

$$KC = \frac{vT}{L} = \frac{2\pi a}{L}. \quad (5)$$

where v is the amplitude of the structures velocity, T is the period of oscillation, and L is the characteristic length of the structure. The second equivalence in Eq. 5 is valid for regular sinusoidal oscillations where a is the amplitude of the oscillation. The drag coefficients are specified for each translational motion of the device, and hence Eq. 5 above, should be valid for each translational mode. Parameterizations of the drag coefficient in heave as a function of KC number for thin plates have shown that the drag coefficients can be quite large (greater than 10) for small KC numbers (less than 0.2) and asymptotically approach drag coefficients of 5 for KC values approaching 1 [7].

As a first estimate, it is reasonable to assume that the device is a perfect wave follower. Based on this assumption, the amplitude of oscillation would be the amplitude of the extreme wave in the heave direction. It could be argued that parallel to the wave direction the relevant amplitude is one half of the wavelength because, to first order, the structure would oscillate according to the velocity of the wave particle kinematics. In the translational mode normal to the wave direction, the device could be considered static. The above postulates require further work to verify their validity; however they offer a method to obtain initial baseline parameters.

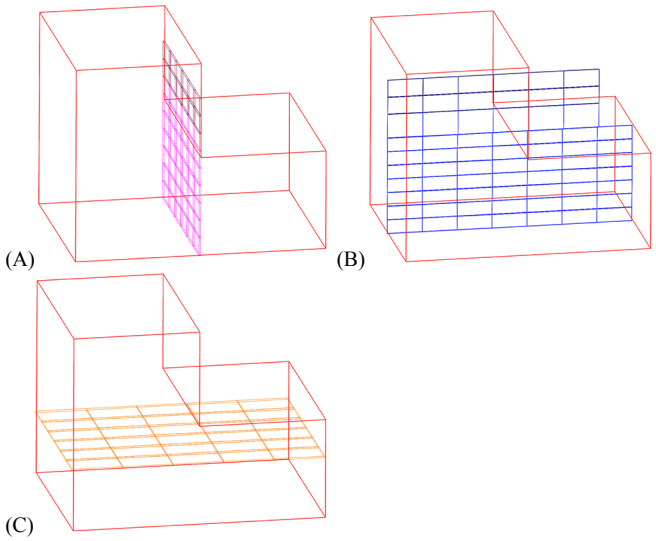

Fig. 4. Surge (A), Sway (B), and Heave (C) Hydrodynamic Bodies: OrcaFlex representation.

Estimates of the drag coefficients are typically refined through experimental tests, as well as considering the effects of the mooring lines on the KC value. More than likely, the device will not be a perfect wave follower and so the KC estimates obtained from this method will be larger than the wave follower KC numbers. In addition, it is unlikely that there is available drag coefficient data parameterized as a function of KC number for the device being modeled. Thus, parameterized studies for drag coefficient are important to fully scope the system parameters.

The heave hydrodynamic bodies are discretized in the x–y plane, the surge hydrodynamic bodies in the y–z plane, and the sway hydrodynamic bodies in the x–z plane. Figure 4 shows the surge (A), sway (B), and heave (C) discretizations. This discretization strategy allows the rotational forces (pitch, roll, and yaw) to be calculated from these translational inputs. This is considered important as estimation strategies for rotational values of drag and added mass coefficients are hard to find in literature and those that do exist (e.g., [8,9]) are only for the most basic of shapes. The discretization method also accounts for changing water particle kinematics, inclusive of any current, with water depth and therefore better represents viscous drag loads.

The translational hydrodynamic loads can now be calculated according to:

$$\boldsymbol{F} = \sum_{j=1}^{N} \left(\boldsymbol{f}_{inertial} + \boldsymbol{f}_{drag} \right)_j \qquad (6)$$

where bolded values should be understood to be a vector composed of the translational directions x, y, and z. The hydrodynamic moment is simply the cross product of position with force:

$$\boldsymbol{M} = \boldsymbol{r} \times \boldsymbol{F} \qquad (7)$$

where $\boldsymbol{r}=[x_j\ y_j\ z_j]$ is the position vector pointing from the reference body to the center of each discrete body and $\boldsymbol{F}$ is the translational hydrodynamic load vector in Eq. 6.

Selection of the appropriate location to center the heave, surge, and sway hydrodynamic bodies will influence the loads on the structure because the water particle kinematics are locally determined. An estimation of the true structure dynamics can be obtained by assigning all hydrodynamic loads to three translational planes only. As shown in Figure 4 the surge (A) and sway (B) hydrodynamic bodies are geometrically centered to represent geometrically averaged affects. Due to the variable submergence of WEC devices in extreme environments, the surge and sway hydrodynamic bodies are continued above the still water line in the same manner as the structural bodies and freely flooding bodies. Figure 4 also shows the heave hydrodynamic bodies (C) are centered at mid-draft, again to attempt to capture geometrically averaged affects.

Neither the added mass nor the drag coefficients are treated as frequency dependent parameters in this study.

D. Full Integration.

A reference body acts as the integrand of the loading effects from each of the discrete body sets. thus allowing the motions to be calculated in 6-DOF. The reference body has no first-order or second-order excitation forces associated with it from potential flow; all motions of the vessel will result from integrated individual loads from the structural bodies, freely flooding bodies, and hydrodynamic bodies.

The reference body also provides the mechanism through which wind loading can be included. Drag-type forces, the second terms in Eq. 4, are used for estimating the mean wind forces. The wind force calculations are directionally dependent and are a function of the shape and height of the structure above the still-water line. Wind (drag) coefficients from scale test data or reference texts can be used in these calculations.

III. CASE STUDY

The method outlined in Section II was applied to a BBDB in order to obtain mooring load estimates in an extreme wave environment. The selected extreme climate is consistent with the conditions representative of a near shore Northern California deployment Table 1 [10].

TABLE I. EXTREME WAVE CONDITIONS [10].

	Depth	59.6	[m]
Spectral Parameters	Significant Wave Height	11.22	[m]
	Peak Period	17.26	[sec]
	Spectrum	JONSWAP or Bretschneider	
Sinusoid Equivalent	Equivalent Wave Height	21.3	[m]
	Period	17	[sec]
	Wave Type	5th order Dean Stream	
	100 yr Wind at 10[m] above SWL	29.6	[m/s]
	Wind Profile	constant	
	10yr Surface Current	0.33	[m/s]
	Current Profile	linear decrease to zero	

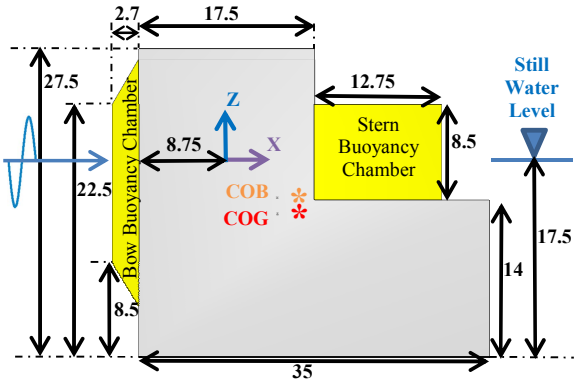

Fig. 5. Structural representation of device showing the major dimensions. (Not shown is the 27 m width of the device.)

TABLE II. STRUCTURAL PROPERTIES OF THE BBDB.

Structural Mass [kg]		2056940		
Bow Buoyancy [m^3]		802		
Stern Buoyancy [m^3]		1205		
Entrained Water [m^3]		14884		
COG (x,y,z) [m]		5.05	0.00	-4.74
COB (x,y,z) [m]		5.05	0.00	-3.27
Inertia at COG [kg*m^2]	x	3.4E+08	0.0	0.0
	y	0.0	4.4E+08	0.0
	z	0.0	0.0	4.5E+08

A. Backward Bent Duct Buoy

The relevant structural parameters of the BBDB being modeled within OrcaFlex are outlined in Figure 5 and Table 2. The data in Table 2 was obtained from a solid model of the device.

Considering the wave climate in Table 1, the diffraction parameter, $\frac{\pi*35}{354} = 0.31$, is small and the waveheight to characteristic length ratio, $\frac{21.3}{35} = 0.61$, for this device is large. Hence, using Morison's Equation as the governing wave-force equation in this extreme environment is valid.

TABLE III. DISCRETIZATION SPECIFICATION FOR BOW AND STERN BUOYANCY CHAMBERS AND FREELY FLOODING BODIES.

Structural and Freely Flooding Bodies			**# bodies** [--]		**Body Specification Radius or x** [m]	**y** [m]	**z** [m]	**Volume/Body** [m^3]	**Total Volume** [m^3]	
Bow Buoyancy	Equilibrium Submerged	main	36	42	2.7	4.5	1.5	18.2	656.1	801.9
		end	6		1.35	4.5	4	24.3	145.8	
	Superstructure	main	30	36	2.7	4.5	1.5	18.2	546.8	692.6
		end	6		1.35	4.5	4	24.3	145.8	
Stern Buoyancy	Equilibrium Submerged		36		2.125	4.5	3.5	33.5	1204.9	
	Superstructure		36		2.125	4.5	5	47.8	1721.3	
Entrained Water Volume	Equilibrium Submerged	horizontal	12		3.54		14	551.2	6614.0	14881.6
		vertical	12		3.54		17.5	689.0	8267.5	
	Superstructure	horizontal	0		--		--	--	--	4724.3
		vertical	12		3.54		10	393.7	4724.3	

TABLE IV. EQUIVALENT RADIUS CALCULATION FOR NONENTRAINED ADDED MASS.

	Projection Area [m^2]	Equivalent Radius [m]	Hemisphere Added Mass [kg]
Heave	945.0	17	11199674
Surge	472.5	12	3959683
Sway	595.9	14	5607773

Data from a solid model was available, thus the mass and inertia of the structure is prescribed at a single 6-DOF lumped buoy located at the mass center of the device. The properties of the mass body consist of structural mass and inertia only. The distributed buoyancy portion of the 'structural bodies' is modeled using an array of 6-DOF lumped buoys in OrcaFlex. The properties of the lumped buoy consist of volume only.

The freely flooding bodies are modeled using a single segment free-flooding line in OrcaFlex. The lines were given an inner and outer diameter (allowing for minimal thickness) and the only property taken into account was the variable mass of the water in the pipe.

Table 3 outlines the discretization for the bow and stern buoyancy chambers as well as the freely flooding components. The total volumes in Table 3 of the equilibrium submerged buoyancy chambers and the freely flooded lines are consistent with the overall device properties in Table 2.

The 'hydrodynamic bodies' are also modeled using 6-DOF lumped buoys with the appropriate Morison Equation parameters, namely projected area, drag coefficient, and added mass. The radius of the hemisphere used to represent the hydrodynamic added mass is based on the projected area of each translational motion as outlined in the following two equations:

$$Radius = \sqrt{\frac{Projected\ Area}{\pi}} \tag{8}$$

$$Added\ Mass = \frac{\rho}{2}\left(\frac{4\pi}{3}(Radius)^3\right). \tag{9}$$

The projection area, equivalent radius, and calculated added mass for this BBDB are presented in Table 4.

TABLE V. DISCRETIZATION AND PROPERTY SPECIFICATION FOR EQUILIBRIUM SUBMERGED AND SUPERSTRUCTURE HYDRODYNAMIC BODIES.

Hydrodynamic Bodies		# bodies --	Added Mass/Body [kg]	Equilibrium Added Mass [kg]	Area/Body [m^2]	C_D/body --	Total Area [m^2]
Heave	Equilibrium Submerged	30	373322	11199660	31.5	5	945.0
	Superstructure	0	--	--	--	--	--
Surge	Equilibrium Submerged	42	94278	3959676	11.25	1.2	472.5
	Superstructure	12	94278	1131336	11.25	1.2	135.0
Sway	Equilibrium Submerged Duct	49	95000	4655000	10	1.2	490.0
	Equilibrium Submerged Buoyancy	6	195000	1170000	17.64	1.2	105.8
				5825000			595.8
	Superstructure	12	120000	1440000	12.6	1.2	151.2

The heave KC number for a perfect wave follower in a 21.3 m regular wave is approximately 2 (from Eq. 5). Using [7], the KC number is low suggesting a large drag coefficient. A drag coefficient of 5 was selected as a baseline for the heave direction. A KC number of 32 is computed from Eq. 5 using the assumption of a perfect wave follower in the surge direction. A KC number of this magnitude indicates that the device appears stationary compared to the oncoming flow. Thus a baseline C_D value of 1.2 was selected for the surge and sway directions.

Table 5 outlines the baseline properties of the hydrodynamic bodies as well as the discretization for each translational direction. The total or integrated added mass in Table 5 is consistent with the appropriate heave and surge added mass in Table 4. In this case, the sway direction integrates to a 4% larger total added mass than the modeled hemisphere of water. The sum of the discrete body projected areas in each direction in Table 5 also matched the overall projected areas in Table 4. Thus, the above drag factors can be applied to each body without modification.

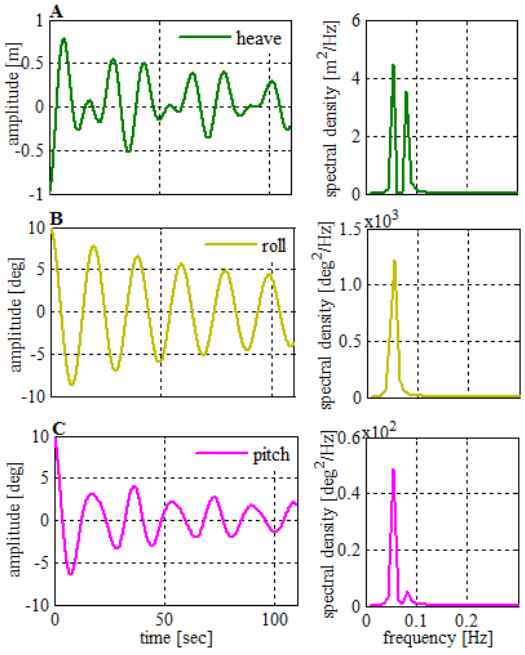

Fig. 6. OrcaFlex decay test results for heave, roll, and pitch initial displacements.

A vessel in OrcaFlex acts as the reference body which integrates the effects from all the discrete bodies outlined in Tables 3 & 5. In addition, the vessel allows for directional wind loading. American Bureau of Shipping rules were used to compute wind drag coefficients for the hull shape above the still water line [11].

The adequacy of this representation of the BBDB is demonstrated by comparison of the natural resonance periods in heave, roll, and pitch from the discrete body array with those obtained from potential theory. The resonance periods were found through small displacement decay tests in OrcaFlex. Time traces of the heave, roll, and pitch decay tests as well as the frequency response are shown in Figure 6.

A numerical comparison of the uncoupled natural periods is shown in Table 6. It is evident that the roll natural period does not compare well. This is attributed to a coarser discretization of buoyant and hydrodynamic bodies in the sway direction which does capture the time dependent variation in water plane area. Sufficient discretization is clearly necessary to obtain good fundamental response.

The results presented in Figure 6 can also be used to assess heave, roll, and pitch damping effects at resonance. However, these affects are relevant to operating conditions where the resonant period may be encountered. Damping is of lesser importance for extreme condition response and is not therefore presented in this paper.

B. Mooring System.

The operational wave climate at the case study site is highly directional. Consequently, the moorings for the BBDB aligned the device to the prevailing operational environment so that power generation can be maximized (Figure 7). The forward port and starboard lines are separated by 60° and the aft line is separated by 150° from both the port and starboard lines.

TABLE VI. COMPARISON OF PREDICTED AND MEASURED NATURAL PERIODS.

	Predicted T [sec]	OrcaFlex T [sec]
Heave Resonance	16.11	18.35
Roll Resonance	11.86	18.35
Pitch Resonance	11.64	11.42

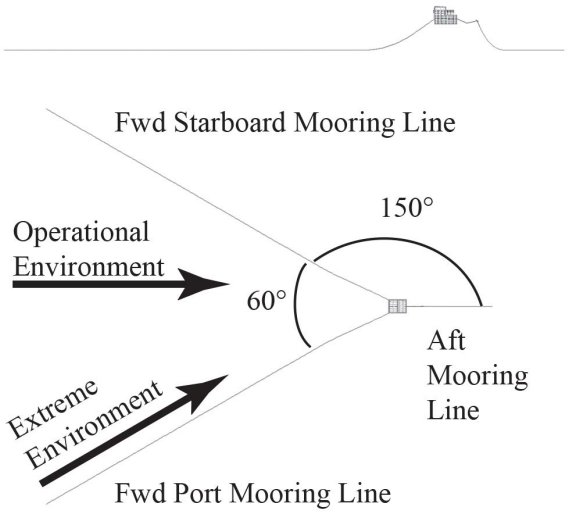

Fig. 7. Elevation and plan views of the BBDB mooring system.

The extreme environment was assumed to consist of collinear wind, wave, and current loads and the mooring system components were sized on the basis that the environment was in line with the forward port mooring line. This approach is consistent with recommended industry practice [12] and accounts for directional variation between operating and extreme conditions.

Tables 7 and 8 detail the mooring system components. Each mooring line is composed of 58 mm R4 Studlink Chain and 137 mm polyester 12 plait synthetic line. The synthetic line is used to add compliance to the system. A 1 Te sinker weight and a 4 Te buoyancy module are attached to the aft mooring line to eliminate snatch loading. These are located 17.5 m at 35 m from the BBDB, respectively.

Figure 8 shows the motions of the BBDB with the baseline hydrodynamic parameters detailed in Table 5 when subject to the extreme conditions collinear with the forward port line. The motions of the device shown in Figure 8 indicate that the assumption of the device being a perfect wave follower for the heave direction is reasonable. However, the surge and sway motions are highly truncated from the wave follower assumption. Figure 8 shows the device drifting back to a new equilibrium position and then oscillating with meters of amplitude around that position. This small oscillation results in much smaller KC values of around 0.5, suggesting that the translational drag coefficients may need to be larger for these directions.

The peak load in the port mooring line is 2089 kN resulting in a factor of safety (FOS) in the chain of 1.74 and 2.75 in the polyester rope.

TABLE VII. MOORING SPECIFICATION.

		Port	Starboard	Aft
Total Length	[m]	810	810	200
Polyester length	[m]	45	45	45
Chain length	[m]	765	765	155
Top Declination Angle	[deg]	122.8	122.8	113.9
Pre Tension	[kN]	110.4	110.4	18.4

TABLE VIII. MOORING LINE PROPERTIES.

			polyester 12 plait	R4 studlink chain
Diameter		[mm]	137	58
mass/unit length		[kg/m]	12	74
Min Breaking Load		[kN]	5754	3628
Drag Coefficient	normal	[--]	1.2	1
	axial	[--]	0.008	0.4
Added Mass Coefficient	normal	[--]	1	1
	axial	[--]	0	0.07
Axial Stiffness		[kN]	138000	339764

An initial assessment suggests that a Vryhof 5 Te Stevpris Mk6 type drag embedment anchor [13] would be necessary to anchor the mooring lines. In reality, site-specific geotechnical information would be required to fully define the anchor specification.

C. Parametric Drag Study.

The baseline case study results are heavily influenced by the selection of Morison Equation drag coefficients. This influence was investigated by parametric study. Knowledge of the parameter influence on loading magnitude allows the designer(s) to assess cost impact with respect to risk of failure in over sizing mooring components. Although not presented here, an analogous exercise with the added mass parameter should be completed when developing the mooring system design.

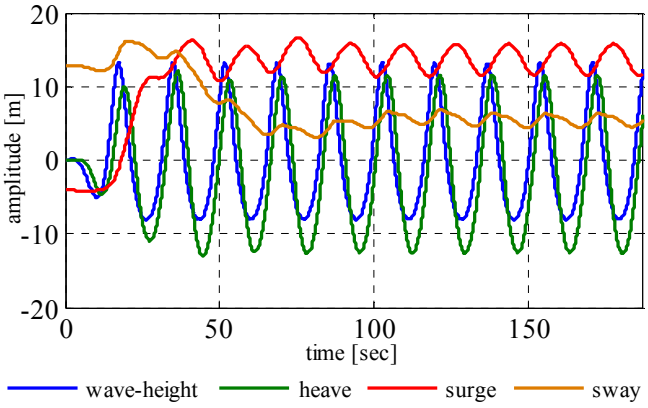

Fig. 8. BBDB motions with baseline hydrodynamic parameters.

TABLE IX. PARAMETRIC DRAG COEFFICIENT STUDY.

Test	C_D Specification Heave	Surge	Sway	Peak Load-Port [kN]
1	5.0	1.2	1.2	2089
2	2.5	1.2	1.2	2651
3	7.5	1.2	1.2	1940
4	5.0	2.5	1.2	3267
5	5.0	5.0	1.2	4894
6	5.0	1.2	2.5	3317
7	5.0	1.2	5.0	4383
8	5.0	2.5	2.5	4311
9	7.5	5.0	5.0	7149

The example parametric drag coefficient study is outlined in Table 9. The load response of the system as the drag coefficient changed in surge or sway was similar, i.e., that cases 4 and 5 resulted in basically equivalent loads to cases 6 and 7 as defined in Table 9. Doubling either the surge or sway drag coefficient (cases 4 & 6) result in approximately a 60% increase in peak load and quadrupling either the surge or sway drag coefficients (cases 5 & 7) results in an approximate doubling in peak load.

The increases in load impact the requirements for the anchors and mooring lines. While still meeting an FOS of 1.5, the results indicate that the initially scoped Mk6 anchor should be increased from 5 Te to 8 Te to 11 Te as the surge (or sway) drag coefficient is increased from 1.2 to 2.5 to 5 with a heave drag coefficient of 5. In addition, these increased loads would require the R4 Studlink Chain to increase in diameter from 58 mm to 70 mm to 81 mm.

Clearly these increases could result in higher material costs and must be considered when selecting the deployment vessels to ensure adequate installation capability. This simple parametric study can assist the developer in better scoping the cost estimates for a particular device.

IV. CONCLUSIONS

A methodology was developed to assess the motions of a WEC device solely using Morison's Equation. The validity of applying Morison's Equation to determine the body motions is dependent upon the magnitude of the diffraction parameter and the waveheight. In extreme waves, these parameters indicate that a Morison's Equation approach is valid.

A BBDB was utilized to illustrate the methodology for the design of a mooring system. Because effects of the PTO can be eliminated when considering extreme conditions, validated mooring time domain solvers, like OrcaFlex, can be readily applied to this problem.

Section II of this paper described the linearization and discretization methodologies adopted to model the BBDB. The linearization is embodied in the separation of modeled phenomena into structural bodies, freely flooded bodies, and hydrodynamic bodies. The structural bodies account for structural mass and inertia, freely flooding bodies account for the time-dependent variation of entrained water mass in the OWC of the device, and the hydrodynamic bodies account for inertial and viscous effects. All these bodies are then connected to one reference body that acts as the integrand of the loading effects.

The discretization methodology adopted addresses three important issues, namely

- time-dependent hydrostatics resulting from variable submergence,
- time-dependent entrained water mass as a result of the device motion, and
- derivation of rotational hydrodynamic characteristics.

Minimizing the number of empirical coefficients for Morison's Equation is advantageous. Allowing the rotational characteristics to be derived from translational input reduces the number of empirical coefficients needed.

The methodology presented in this paper is not specific to the particular WEC design. As long as the wavelength is much larger than the device characteristic length or the wave amplitudes are large in comparison to the device length and the PTO does not have to be modeled for survival conditions, the approach outlined in this paper is valid

Section III of this paper illustrates the methodology developed in Section II. The physical parameters used to model the BBDB for each of the phenomena are detailed and suitability of this representation is demonstrated through comparison of the natural resonance periods in heave, roll, and pitch obtained from potential theory and a time domain solution.

A mooring design is then coupled to the BBDB. The design is subject to the extreme wave along one mooring leg. The presented design has sufficient FOS' for the extreme conditions with baseline parameters assigned to the BBDB.

The importance of the Morison Equation hydrodynamic parameters were assessed by parametric study. This indicated that a doubling of either the surge or sway drag coefficients results in a 60% increase in peak mooring loads. This increase in load mandated an increase in both the chain diameter as well as the anchor size. These changes may have major implications on the WEC design and the total installed cost of the WEC mooring system.

V. ACKNOWLEGMENTS

Sandia National Laboratories is a multiprogram laboratory managed and operated by Sandia Corporation, a wholly owned subsidiary of Lockheed Martin Corporation, for the U.S. Department of Energy's National Nuclear Security Administration under contract DE-AC04-94AL85000.

This research was made possible by support from the Department of Energy's Energy Efficiency and Renewable Energy Office's Wind and Water Power Program.

VI. REFERENCES

[1] T. Whittaker and M. Folley, "Optimisation of wave power devices towards economic wave power systems," World Renewable Energy Congress, Aberdeen, Scotland, September, 2005.

[2] Y. Masuda, "Experience in pneumatic wave energy conversion in Japan," in Proceedings, Utilization of Ocean Waves-Wave to Energy Conversion, ASCE,M.E. McCormick and Y. C. Kim, Eds. pp. 1–33, 1986.

[3] A. F. de O. Falcão, "Wave energy utilization: A review of the technologies," *Renewable and Sustainable Energy Reviews* Vol. 14, no. 3, pp. 899–918, April 2010.

[4] Y. Imai, K. Toyota, S. Nagata, T. Setoguchi, and M. Takao, "An Experimental Study on Generating Efficiency of a Wave Energy Converter 'Backward Bent Duct Buoy'," European Wave and Tidal Energy Conference, Southampton, UK, 2011.

[5] S. K. Chakrabarti, *Hydrodynamics of Offshore Structures*, Southampton, UK, Computational Mechanics Publications, 1987, Chapter 7.

[6] Orcina Limited, OrcaFlex Version 9.5, 2011.

[7] H. He, W. Troesch, and M. Perlin, "Hydrodynamics of damping plates at small KC numbers," Symposium on Fluid-Structure Interaction in Ocean Engineering, Hamburg, Germany, 2008.

[8] J. N. Newman, Marine Hydrodynamics, Cambridge, MA, MIT Press, 1977.

[9] R. D. Blevins, Formulas for Natural Frequency and Mode Shape, Malabar, FL, Krieger Publishing Co., 1979.

[10] J. Berg, "Extreme ocean wave conditions for Northern California wave energy conversion device," Sandia National Laboratories document SAND2011-9304, November 2011.

[11] ABS Guide for Building and Classing Floating Production Installations, Houston, TX, American Bureau of Shipping, May 2000, Chapter 3.

[12] Det Norske Veritas, "Position Mooring," Offshore Standard DNV-OS-E301, 2008. Amended October 2009. Web access 12-Oct-2010.

[13] Vryhof Anchors B.V., Anchor Manual 2010.